TU Delft
Technische Universiteit Delft

Nanomechanics

Yaroslav M. Blanter

Kavli Institute of Nanoscience, Delft University of Technology

- Coupling
- Detection
- Doubly-clamped beams
- Graphene and 2D materials

Mechanical oscillator

Driven harmonic oscillator: $$\ddot{x} + \frac{\omega_0}{Q}\dot{x} + \omega_0^2 x = \frac{F}{M}\cos\omega t$$

$$x = A\cos\left(\omega t + \theta\right)$$

A peak of the amplitude and a jump of the phase

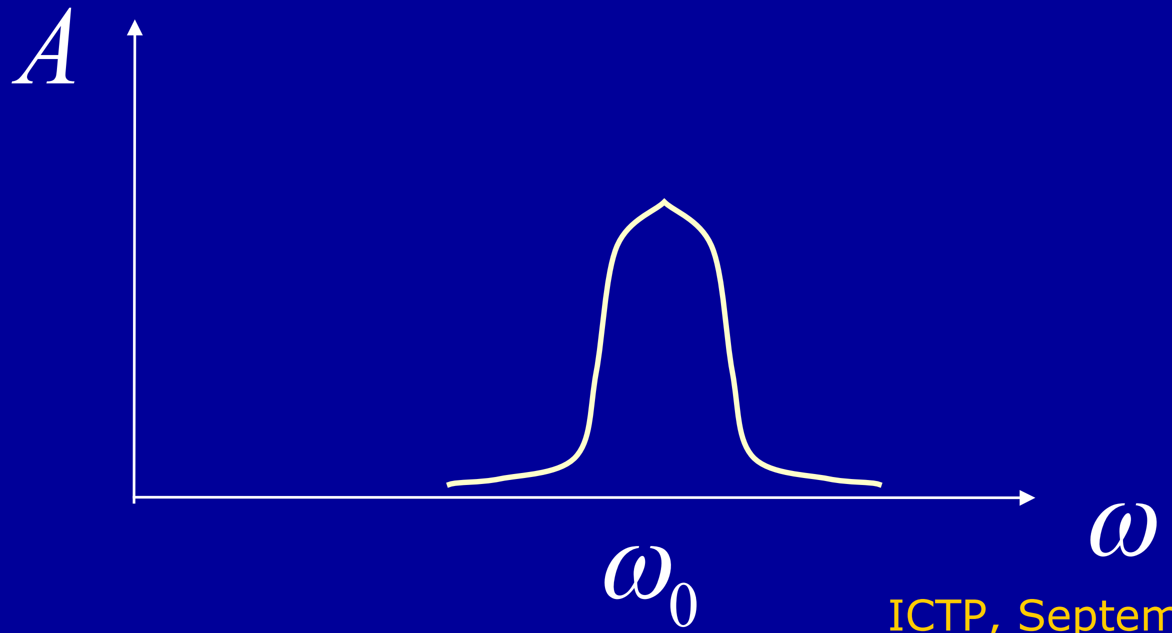

Mechanical oscillator

More advanced oscillator:

$$\ddot{x}+\frac{\omega_0}{Q(x)}\dot{x}+\omega_0^2 x+f(x)=\frac{F(x,t)}{M}$$

$$x \neq A\cos\left(\omega t+\theta\right)$$

Nano- or optomechanical system:

$$\ddot{x}+\frac{\omega_0}{Q(x)}\dot{x}+\omega_0^2 x+f(x)=\frac{F(x,y,t)}{M}$$

and another equation for evolution of y – the degree of freedom to which the mechanical oscillator is coupled

Coupling

Mechanical resonators can be coupled to:

– Charge: capacitive coupling
– EM radiation: radiation pressure coupling
– Spin
– Magnetic flux: inductive coupling
– Other mechanical resonators

Capacitive coupling

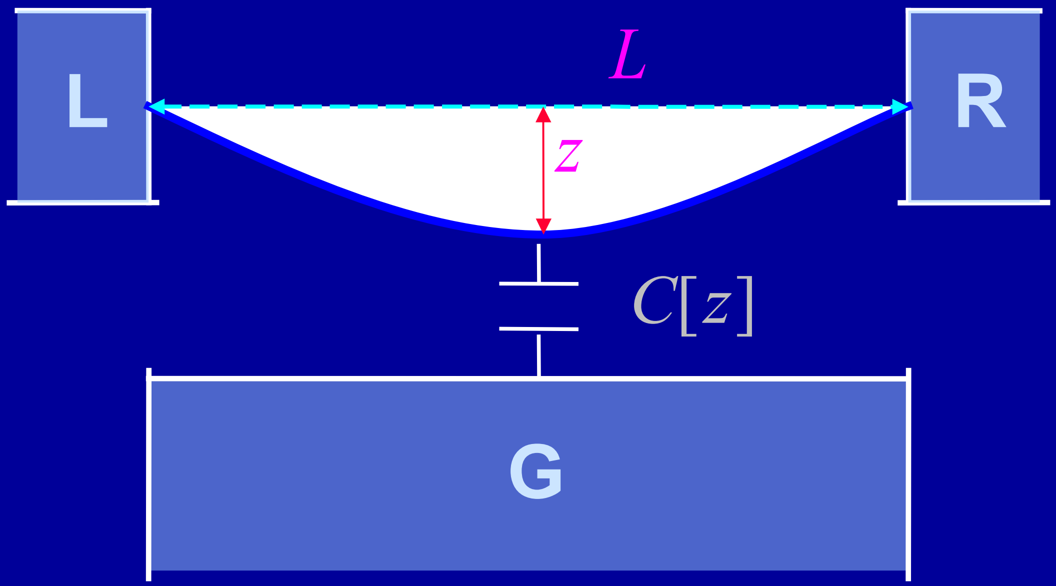

Electrostatic energy:

In the simplest form

$$\frac{Q^2}{2C[z]} = \frac{C[z]V^2}{2}$$

Couples phonons to charge due to the Coulomb-induced force

(Other mechanisms of coupling to the charge: e.g. piezoelectric coupling)

Capacitive coupling

Graphene resonator
on a hole over a backgate

T. Miao, S. Yeom, P. Wang,
B. Standley, M. Bockrath,
Nano Lett. **14**, 2982 (2014)

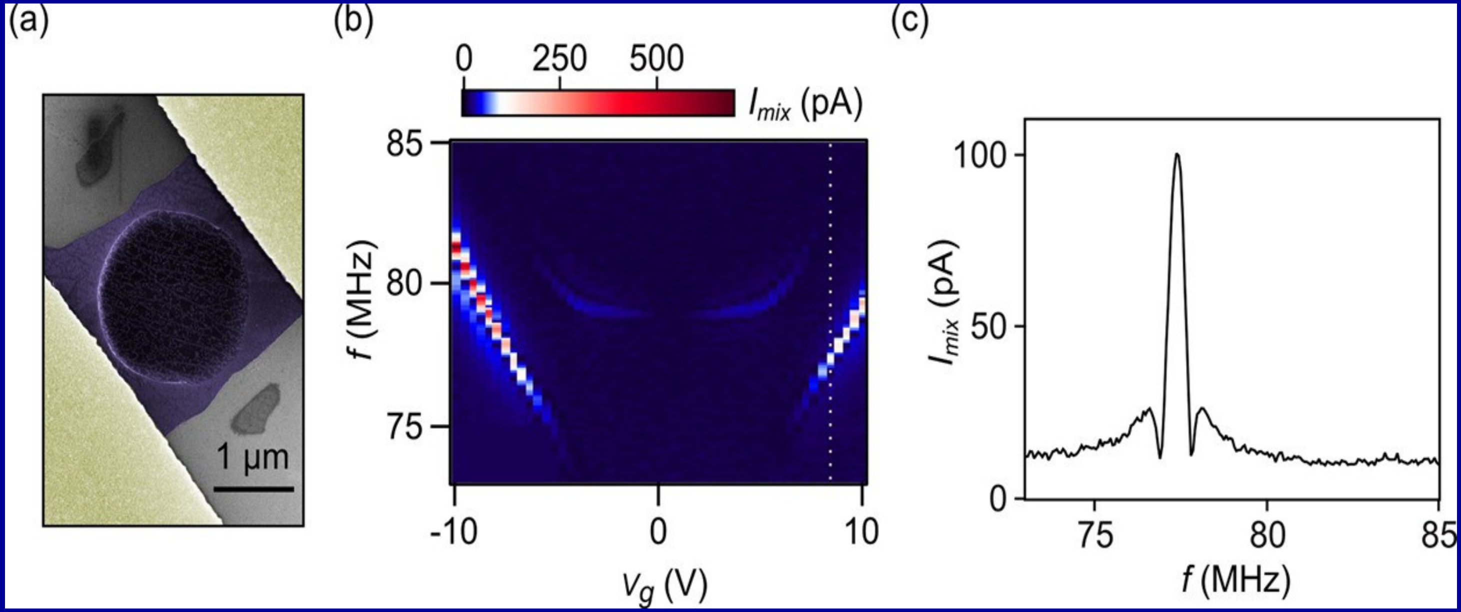

Radiation pressure coupling

Movable mirror

Static mirror

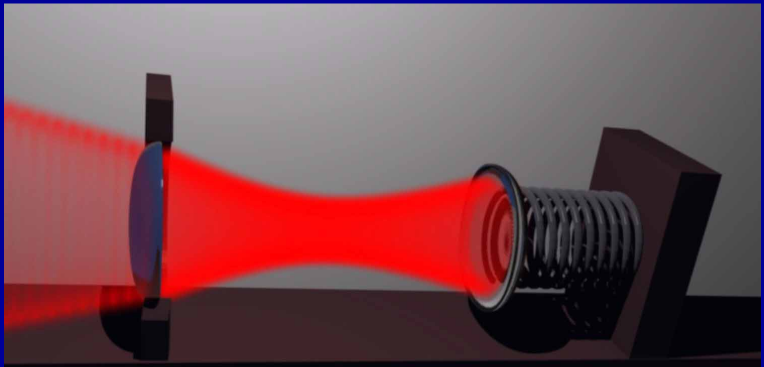

Kippenberg's group website

$$\omega_{cav}(x) \approx \omega_{cav} + \frac{\partial \omega_{cav}}{\partial x} x$$

Radiation pressure: $\frac{\partial \omega_{cav}}{\partial x} \hbar x n$

$$H = \hbar \omega_{cav}(x) n + \frac{M \omega_m x^2}{2}$$

Cavity

Mechanical resonator

Other mechanisms of interaction with radiation: e.g optical phonons in bulk solids

Radiation pressure coupling

S. Hong, R. Riedinger, I. Marinkovic, A. Wallucks, S. G. Hofer, R. A. Norte, M. Aspelmeyer, S. Gröblacher, arXiv:1706.03777

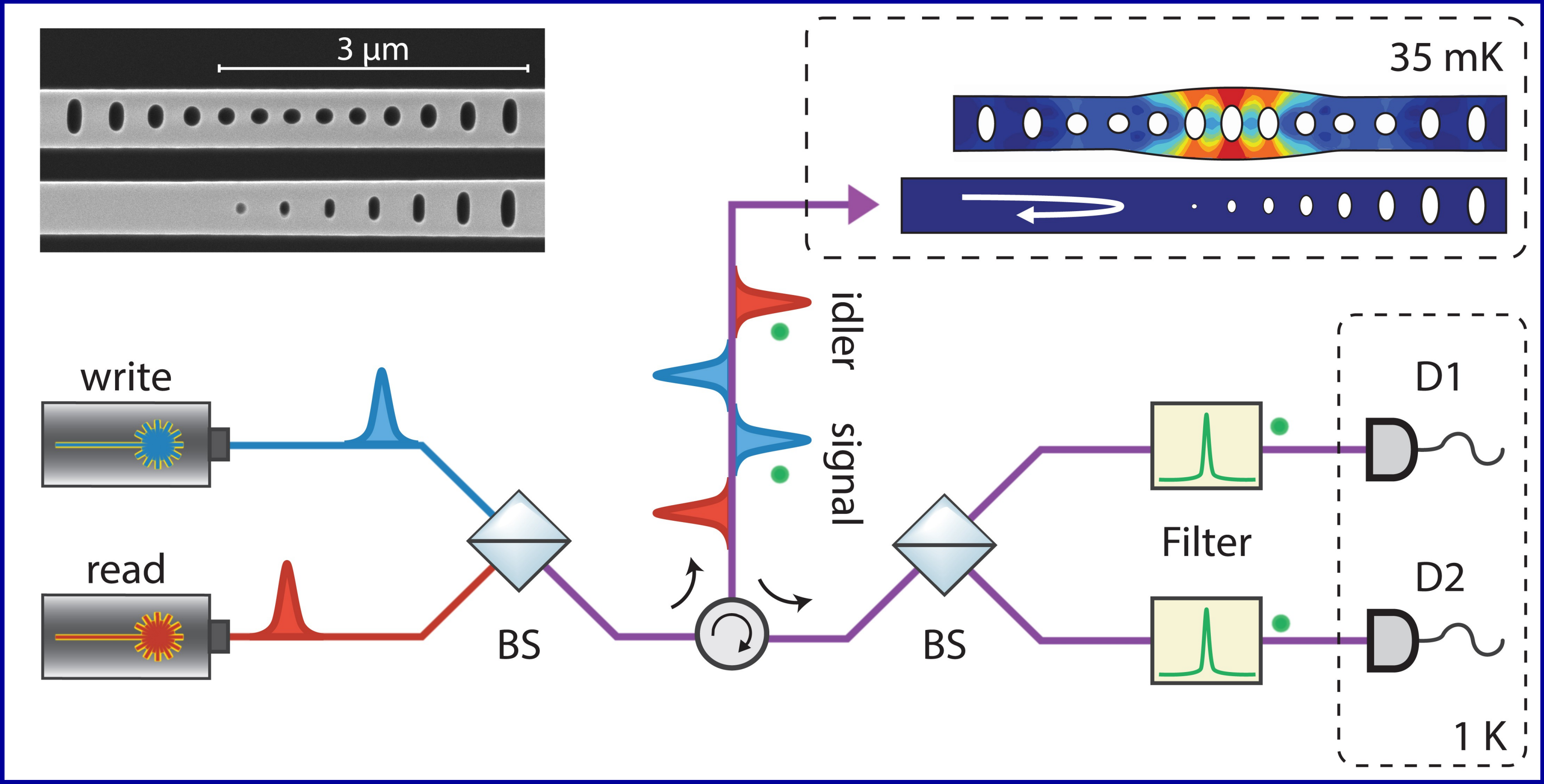

Coupling to spin

Two magnets exert mechanical force on each other, dependent on their orientation

⇓

A magnet on a cantilever can sense a spin

⇓

Magnetic resonance force microscopy

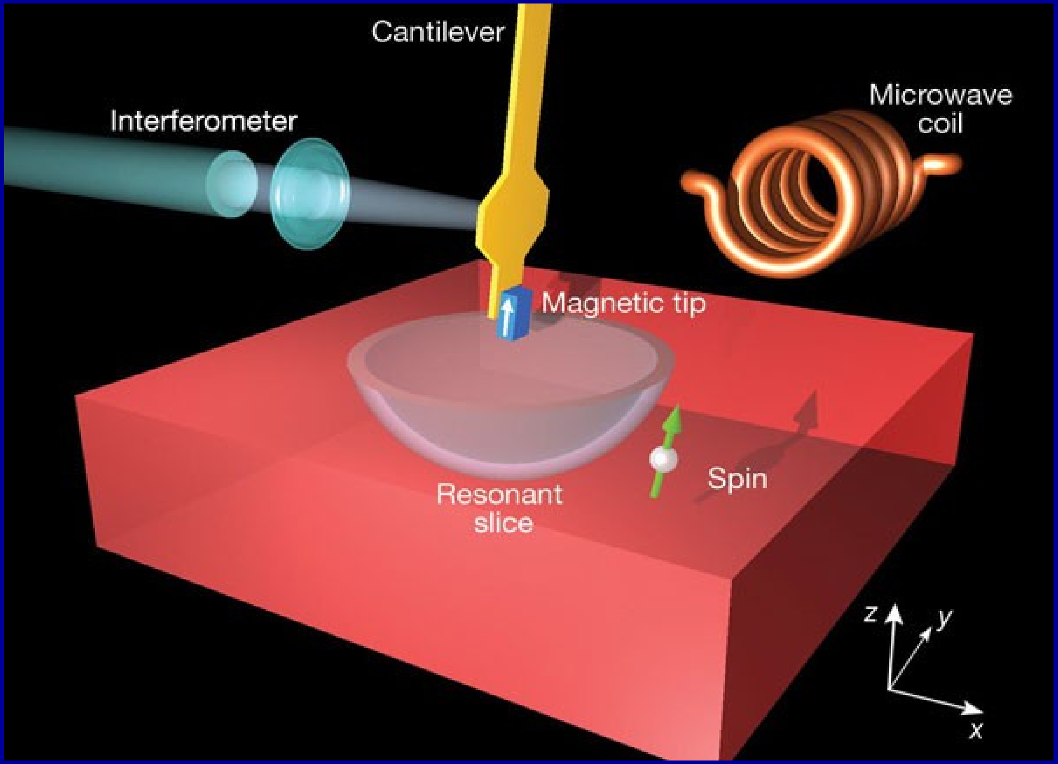

D. Rugar, R. Budakian, H. J. Mamin, B. W. Chui, Nature **430**, 329 (2004)

Coupling to spin

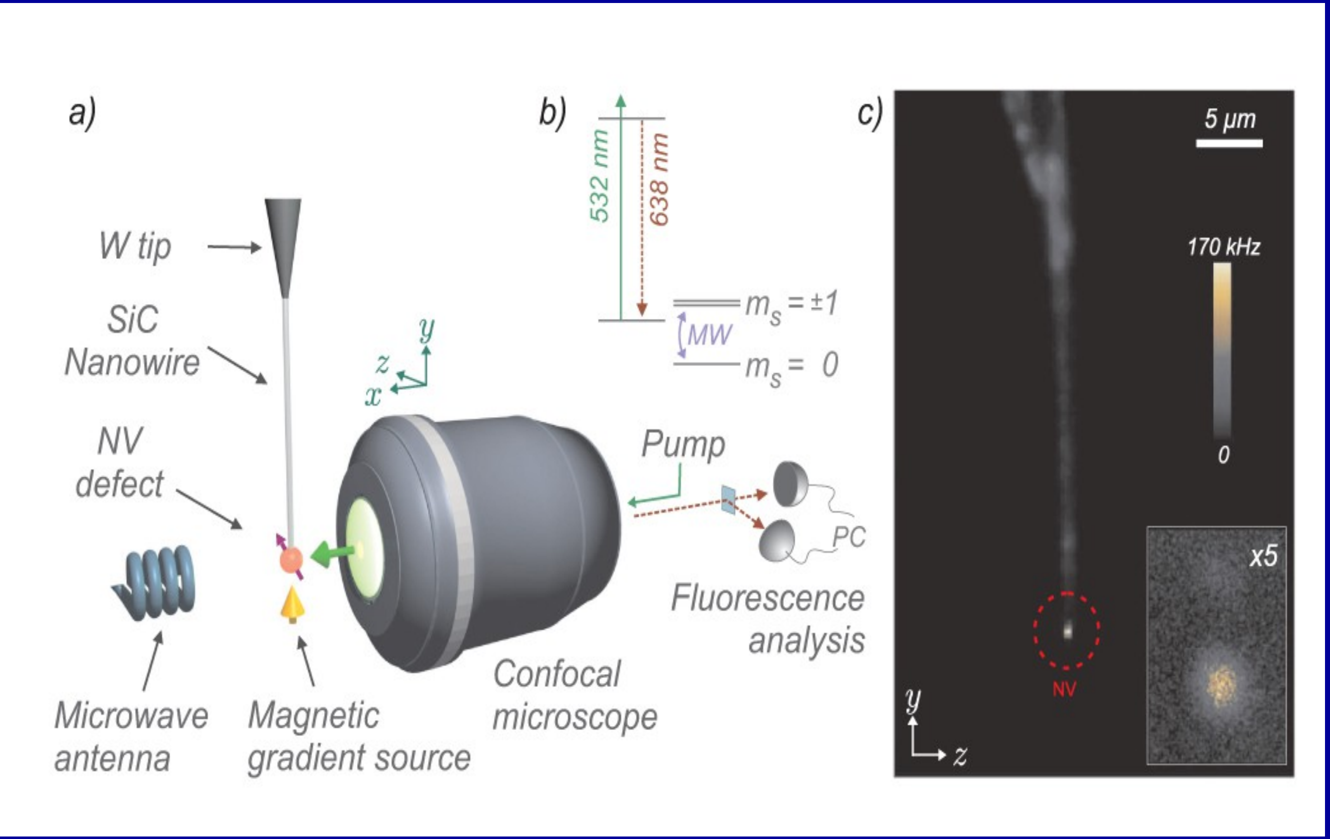

O. Arcizet, V. Jacques, A. Siria, P. Poncharal, P. Vincent, and S. Seidelin
Nature Physics **7**, 879 (2011)

Coherent spin driving

Spin state depends on the strain; piezoelectric substrate driven

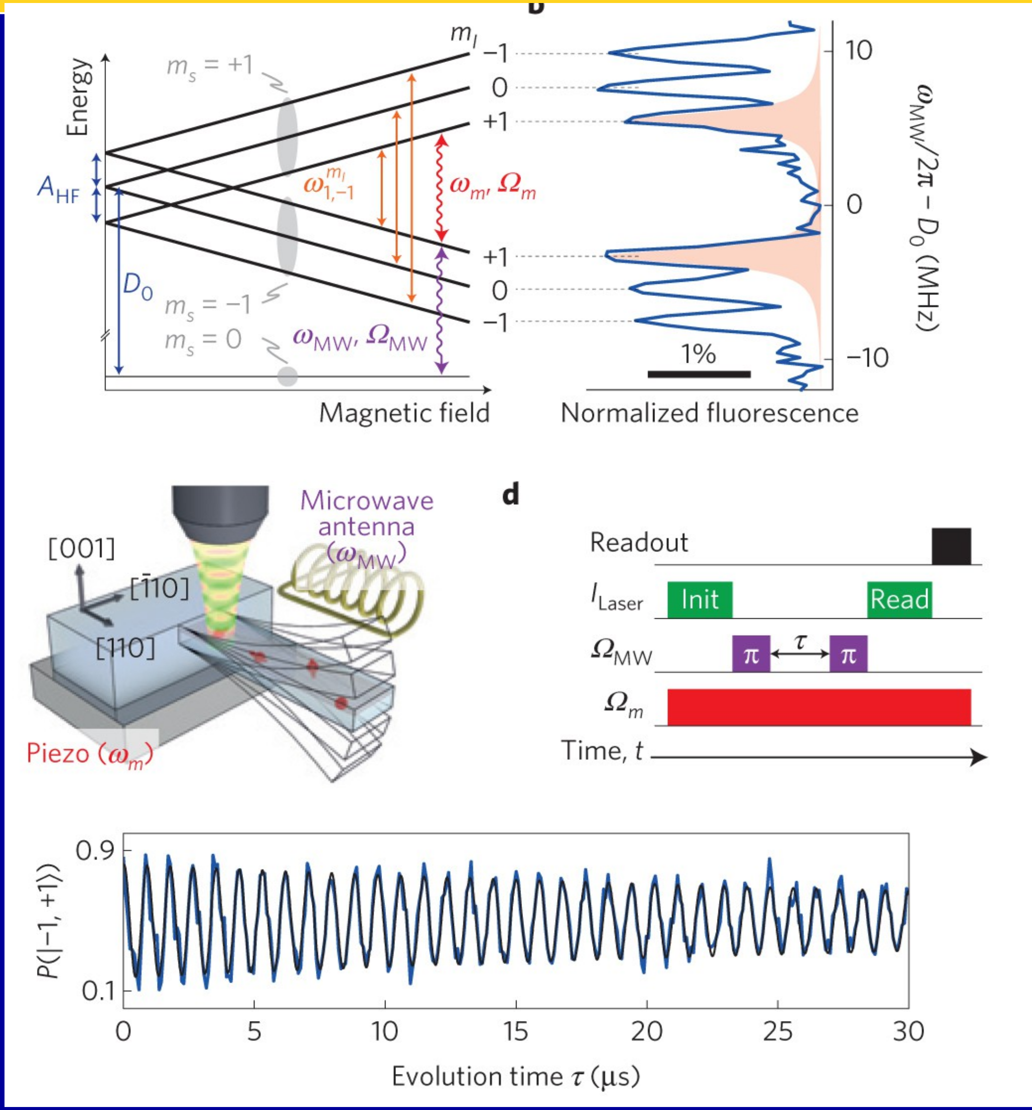

A. Barfuss, J. Teissier, E. Neu, A. Nunnenkamp, P. Maletinsky Nature Physics **11**, 820 (2015)

Inductive coupling

Inductance: can depend on the position of a mechanical resonator

$$\Phi = LI \Rightarrow -\dot{\Phi} = V = L\dot{I}$$

$$E = \frac{L(x)I^2}{2}$$

See Lecture 3

Persistent currents

Interference is affected by Aharonov-Bohm flux

$$\hat{H} = \frac{\hbar^2}{2m}\left(\hat{\vec{p}} - \frac{e}{c}\vec{A}\right)^2 \Rightarrow$$

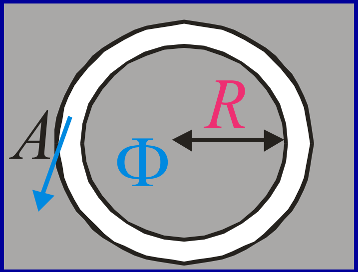

$$\hat{H} = \frac{\hbar^2}{2mR^2}\left(-i\frac{\partial}{\partial\phi} - \frac{\Phi}{\Phi_0}\right)^2 ; \qquad E \Big/ \frac{\hbar^2}{2mR^2}$$

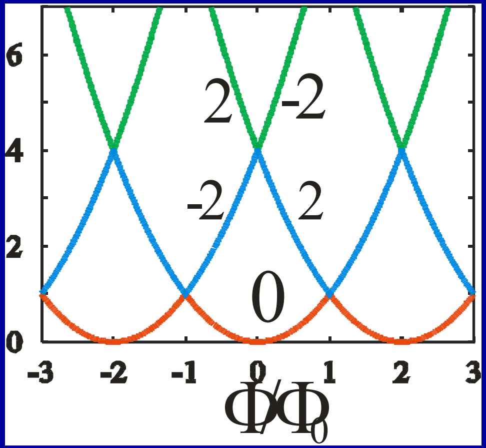

$$\Psi(\phi) \propto e^{iN\phi} \Rightarrow$$

$$E = \frac{\hbar^2}{2mR^2}\left(N - \frac{\Phi}{\Phi_0}\right)^2$$

Energy levels vs. flux

Measurements of persistent currents

$$I = \frac{\partial E}{\partial \Phi} = \sum_{\substack{filled \\ levels}} \frac{\partial E_i}{\partial \Phi}$$

A. C. Bleszynski-Jayich et al, Science **326**, 272 (2009)

Experiments to date have produced a number of confusing results in apparent contradiction with theory and even among the experiments themselves (*2*, *3*). These conflicts have remained without a clear resolution for nearly 20 years, suggesting that our understanding of how to measure and/or calculate the ground-state properties of as simple a system as an isolated metal ring may be incomplete.

Amplitude clean, single ring: $\frac{e\hbar}{mR^2}$

Amplitude disordered:

$$I = \sum_l I_l \sin \frac{2\pi l \Phi}{\Phi_0}, I_l = -\frac{4e\delta}{\pi^2 \hbar}$$

Difficult to measure!

Measurements of persistent currents

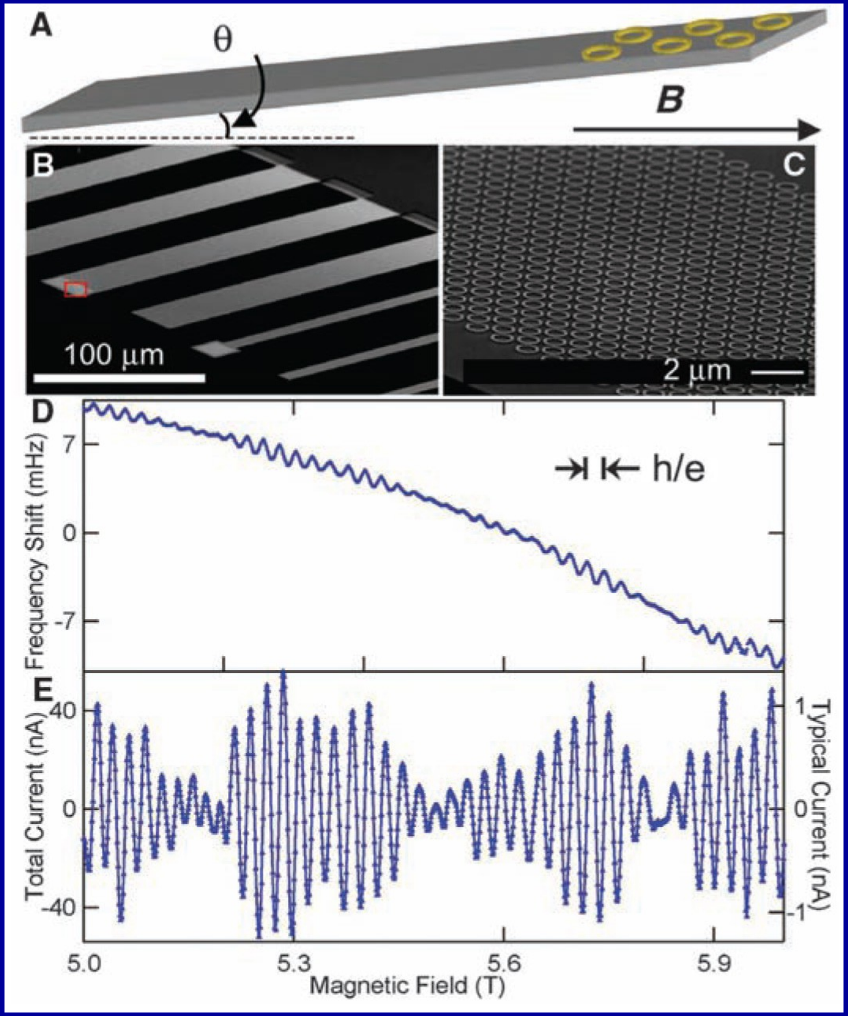

A. C. Bleszynski-Jayich, W. E. Shanks, B. Peaudecerf, E. Ginossar, F. von Oppen, L. Glazman, J. G. E. Harris
Science **326**, 272 (2009)

Currents produce tork and shift the cantilever frequency

$$\tau = \mu \times B$$

Good agreement with the theory predictions

Coherent two-mode manipulation

T. Faust, J. Rieger, M. J. Seitner, P. Krenn, J. P. Kotthaus, E. M. Weig, PRL **109**, 037205 (2012)

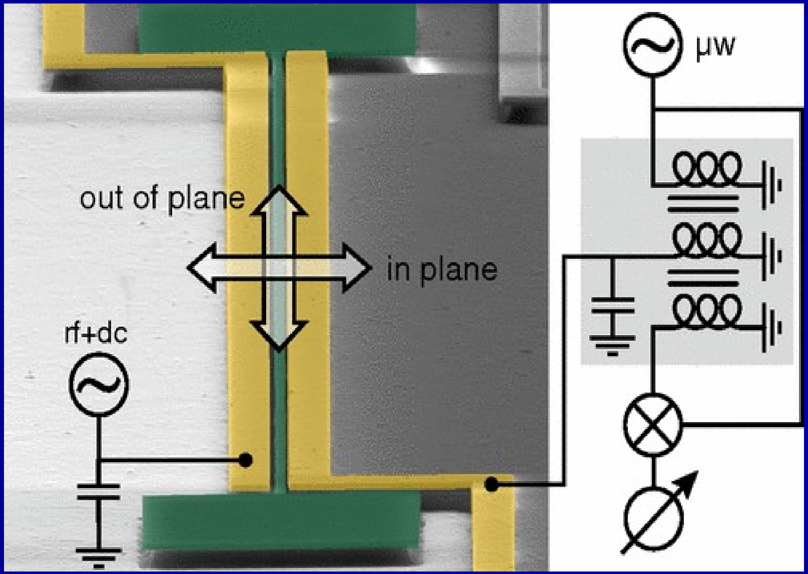

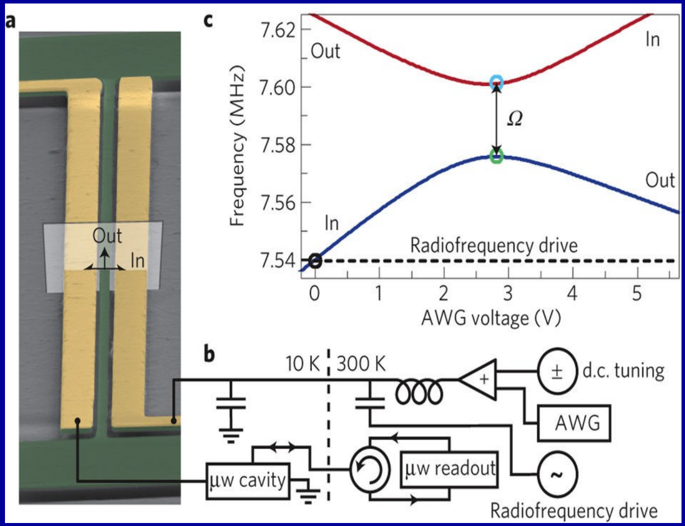

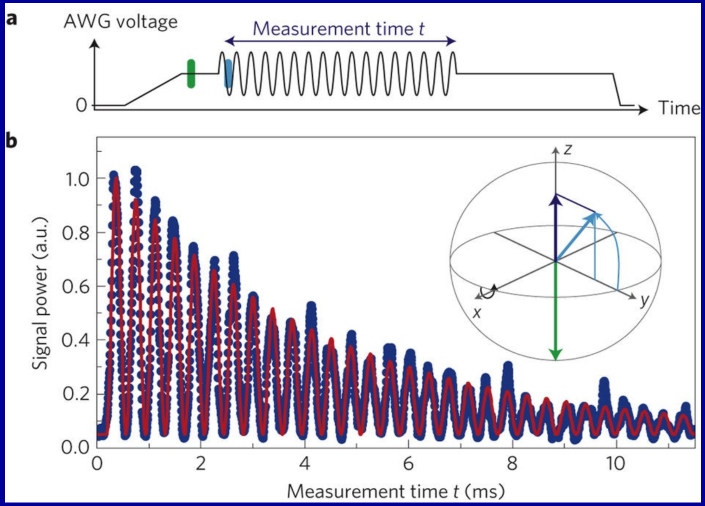

T. Faust, J. Rieger, M. J. Seitner, J. P. Kotthaus, E. M. Weig, Nature Physics **9**, 485 (2013)

Mass detection

Y. T. Yang, C. Callegari, X. L. Feng, K. L. Ekinci, M. L. Roukes,
Nano Letters **6**, 583 (2006)

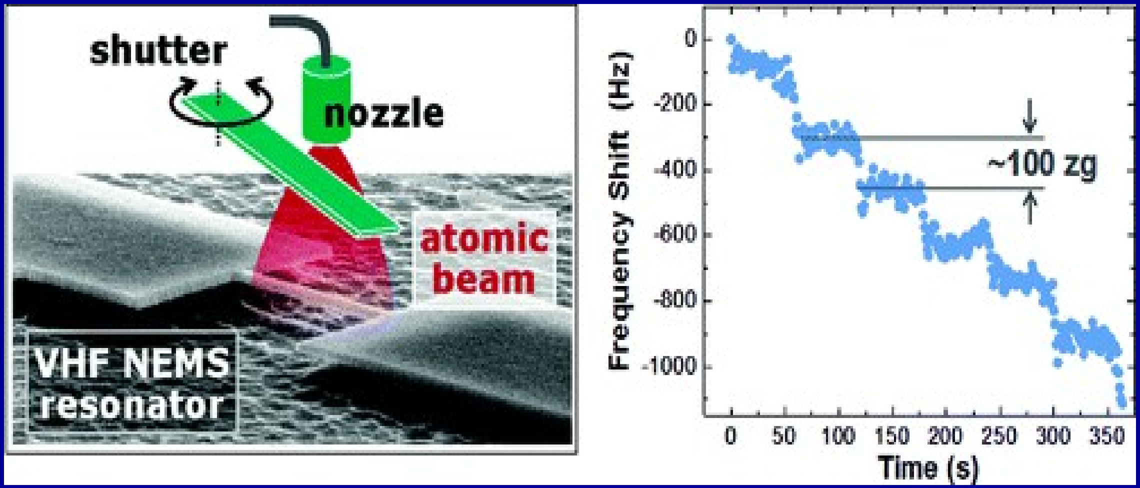

Resonant frequency: 133 MHz
Size: 2300 x 150 x 70 nm
Mass sensitivity: 100 zg

Single-molecule detection

M. S. Hanay, S. Kelber, A. K. Naik, D. Chi, S. Hentz, E. C. Bullard, E. Colinet, L. Duraffourg, M. L. Roukes, Nature Nanotech. **7**, 602 (2012)

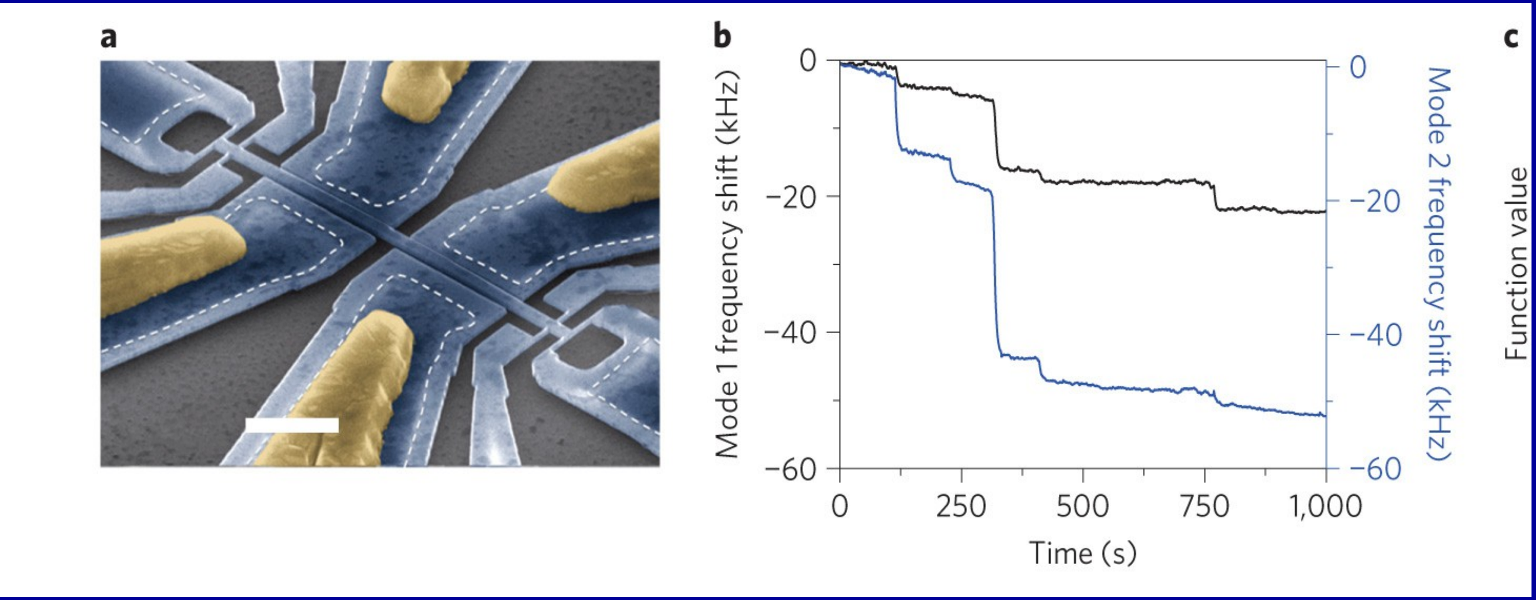

J. Chaste, A. Eichler, J. Moser, G. Ceballos, R. Rurali, A. Bachtold Nature Nanotech. **7**, 301 (2012) – 1 yg resolution

Technische Universiteit Delft

nature physics

ARTICLES

PUBLISHED ONLINE: 12 JANUARY 2014 | DOI: 10.1038/NPHYS2842

Real-space tailoring of the electron–phonon coupling in ultraclean nanotube mechanical resonators

A. Benyamini[1†], A. Hamo[1†], S. Viola Kusminskiy[2], F. von Oppen[2] and S. Ilani[1★]

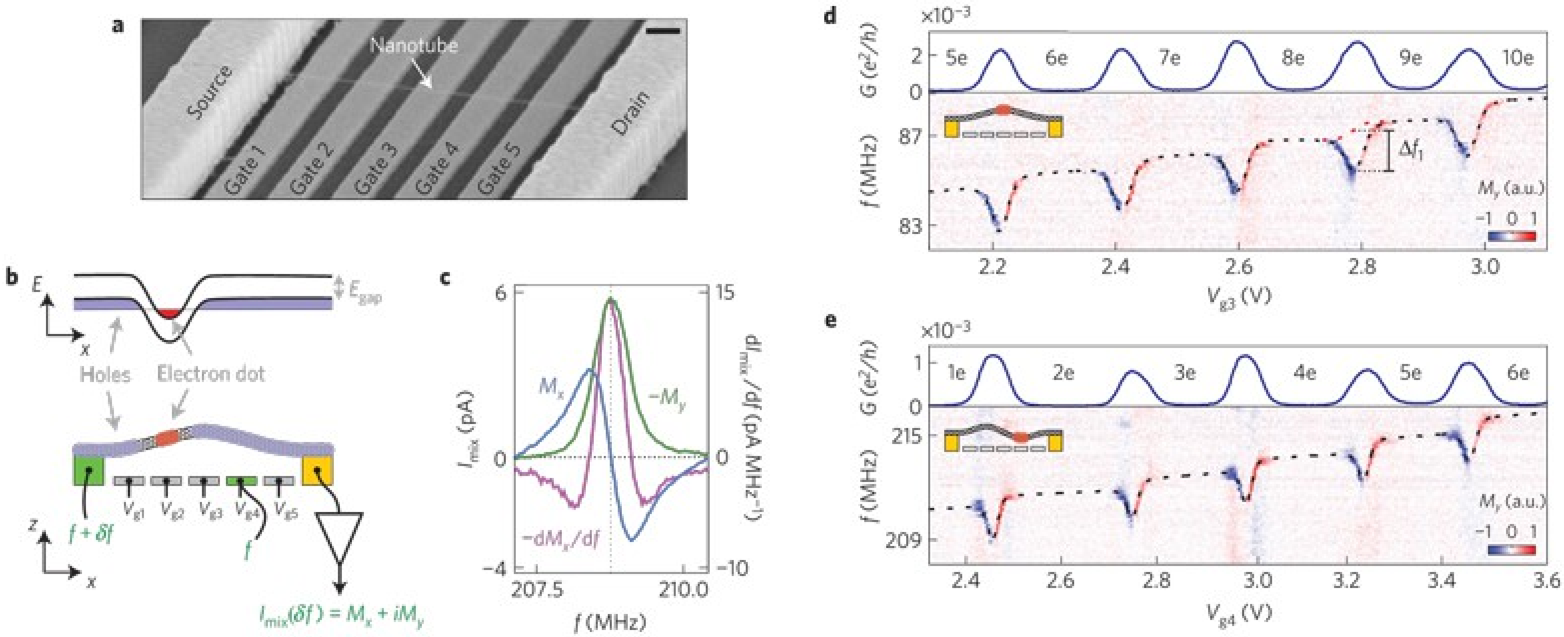

Figure 1 | A carbon nanotube mechanical resonator coupled to localized ultraclean quantum dots. a, Scanning electron micrograph of a device similar to the one measured, with an 880-nm-long nanotube suspended 125 nm above five gates with a periodicity of 150 nm. Scale bar, 100 nm. **b**, Measurement layout: d.c. gate voltages, V_{g1} to V_{g5}, locally dope the nanotube with electrons (red) or holes (blue). Mechanical motion is actuated by a radiofrequency signal on gate 4 (frequency f) leading to a high-frequency modulation of the current, which is down-mixed to low frequencies using a weak probe signal of frequency $f+\delta f$ applied at the source. **c**, The mixing current, which is the current measured at frequency δf, has components that are in-phase (M_x) and out-of-phase (M_y) with the drive; both are plotted as function of the drive frequency (blue and green, respectively). Also shown is the derivative dM_x/df (purple). **d**, Top: conductance, G, of a dot above gate 3 as a function of V_{g3}. Bottom: corresponding mixing signal, M_y (colour map), measured for the first mechanical mode, as a function of V_{g3} and f. Dashed red line is a fit to a theory including only the static electron–phonon coupling, capturing the frequency step across a Coulomb blockade peak. The dashed black line includes also the dynamical coupling (Supplementary Information 1). Their difference at the centre of the Coulomb peak, Δf_1, gives the dynamic frequency softening. **e**, Similar measurement for the second mechanical mode with a dot above gate 4. All measurements in this article are done at an electron temperature of $T = 16$ K as determined from the Coulomb peaks in the conductance.

Double-clamped beam

S. Sapmaz . YMB. L. Gurevich,
H. S. J. van der Zant,
PRB **67**, 235414 (2003)

G. Steele, A. K. Hüttel, B. Witkamp,
M. Poot, H. B. Meerwaldt,
L. P. Kouwenhoven, H. S. J. van der Zant
Science **325**, 1103 (2009)

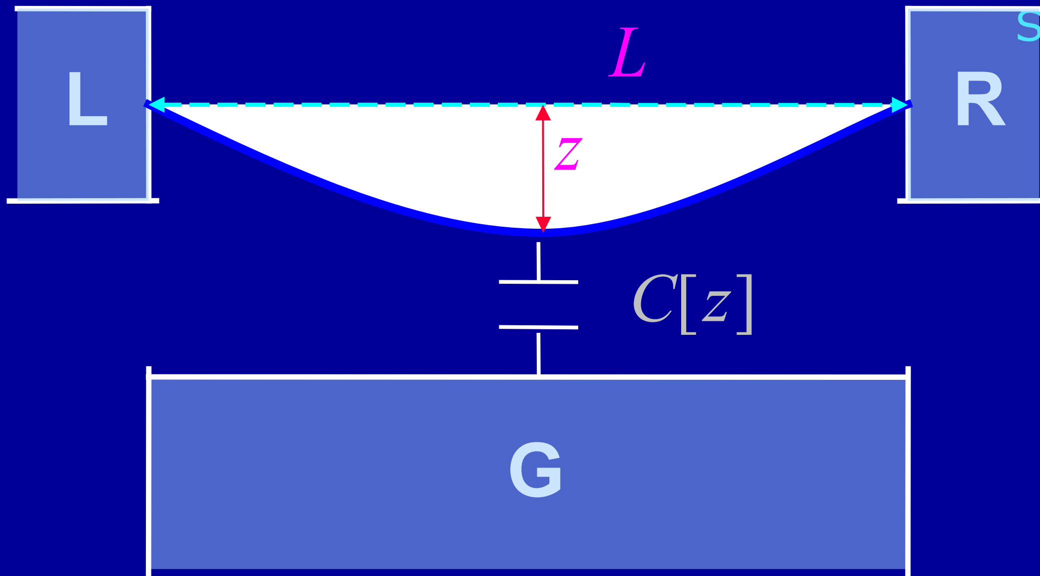

Couples phonons to charge due to the Coulomb-induced force

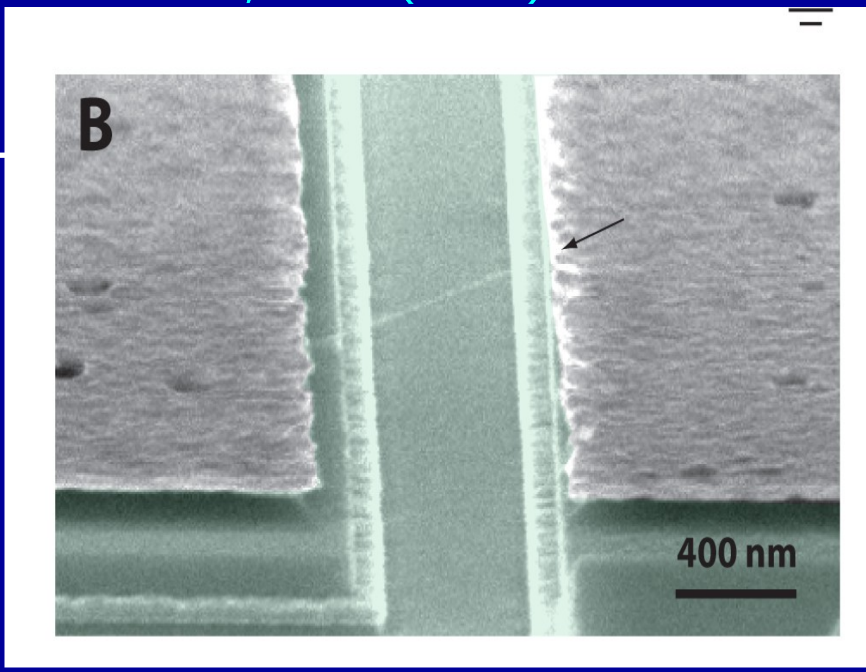

Size: 500 nm
Frequency: 140 MHz

Backaction in a double-clamped beam

H. B. Meerwaldt, G. Labadze, B. H. Schneider, A. Taspinar, YMB, H. S. J. van der Zant, and G. A. Steele, PRB **86**, 115454 (2012)

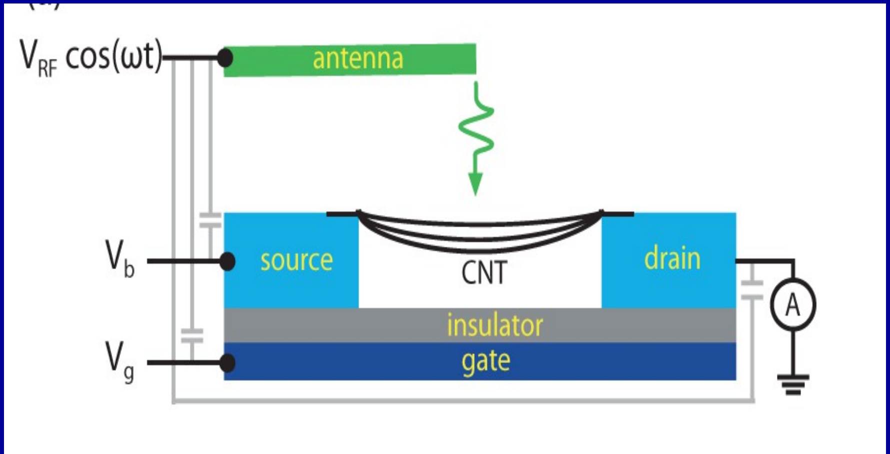

$$M\ddot{x} + \frac{M\omega_0}{Q}\dot{x} + M\omega_0^2 x = F[x]$$

$$F = \frac{1}{2}\frac{d}{dx}C_g(x)\left(V_g - V_{CNT}(x)\right)^2$$

$$F[x] = -\Delta k x - \beta x^2 - \alpha x^3$$

The beam is stretched by the gate voltage, and this shifts the frequency (optical spring effect)

Coulomb blockade

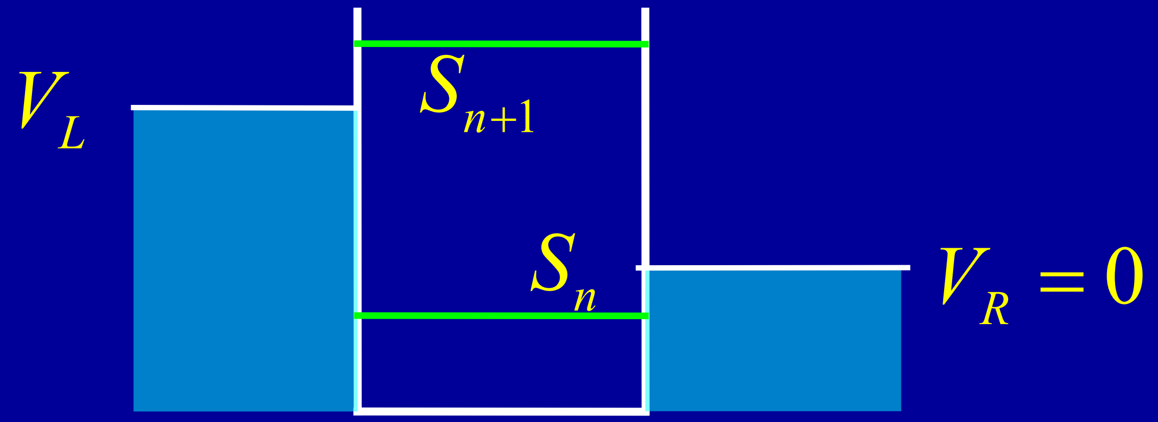

Conditions that current is not flowing:

(a) $S_{n+1} > eV_L$

(b) $S_n < eV_L$

(c) $S_{n+1} > 0$

(d) $S_n < 0$

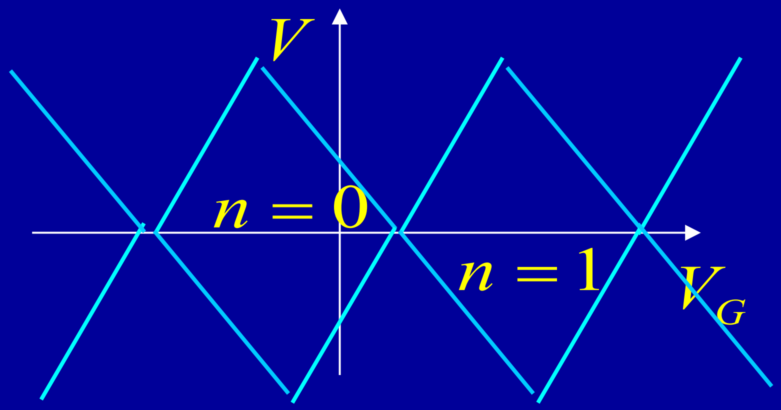

Frequency softening by Coulomb effects

H. B. Meerwaldt, G. Labadze, B. H. Schneider, A. Taspinar, YMB, H. S. J. van der Zant, and G. A. Steele, PRB **86**, 115454 (2012)

$$\Delta\omega_0 \propto 1 - \frac{C_{tot}}{C_g} - \frac{e}{C_g}\frac{\partial\langle N\rangle}{\partial V_g}$$

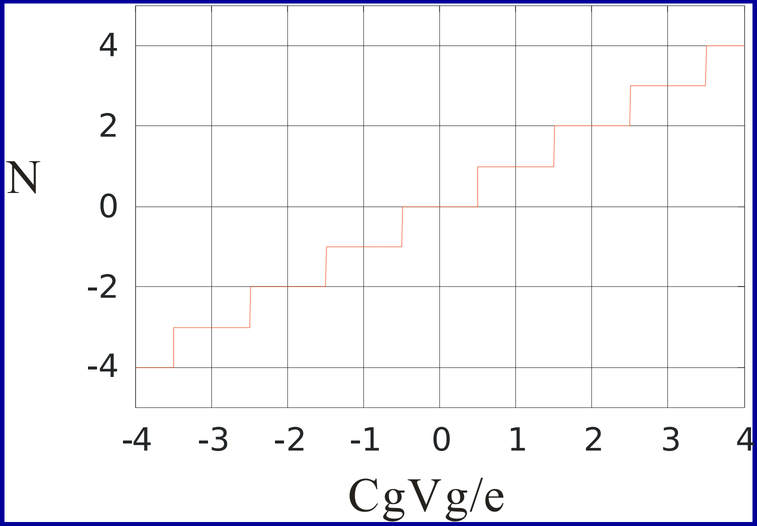

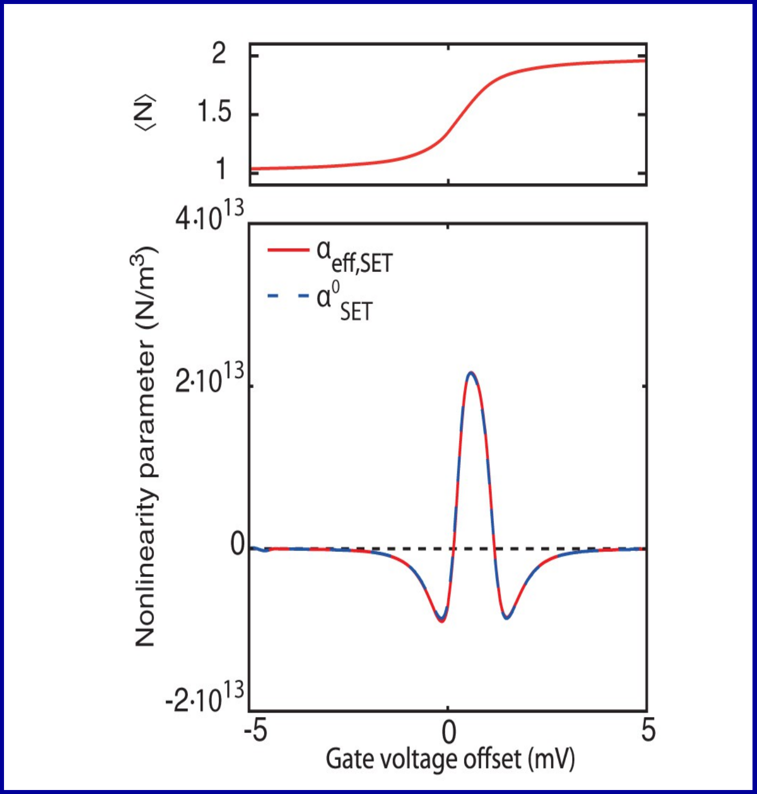

(zero bias)

Frequency softening by Coulomb effects

H. B. Meerwaldt, G. Labadze, B. H. Schneider, A. Taspinar, YMB, H. S. J. van der Zant, and G. A. Steele, PRB **86**, 115454 (2012)

$$\Delta\omega_0 \propto 1 - \frac{C_{tot}}{C_g} - \frac{e}{C_g}\frac{\partial\langle N\rangle}{\partial V_g}$$

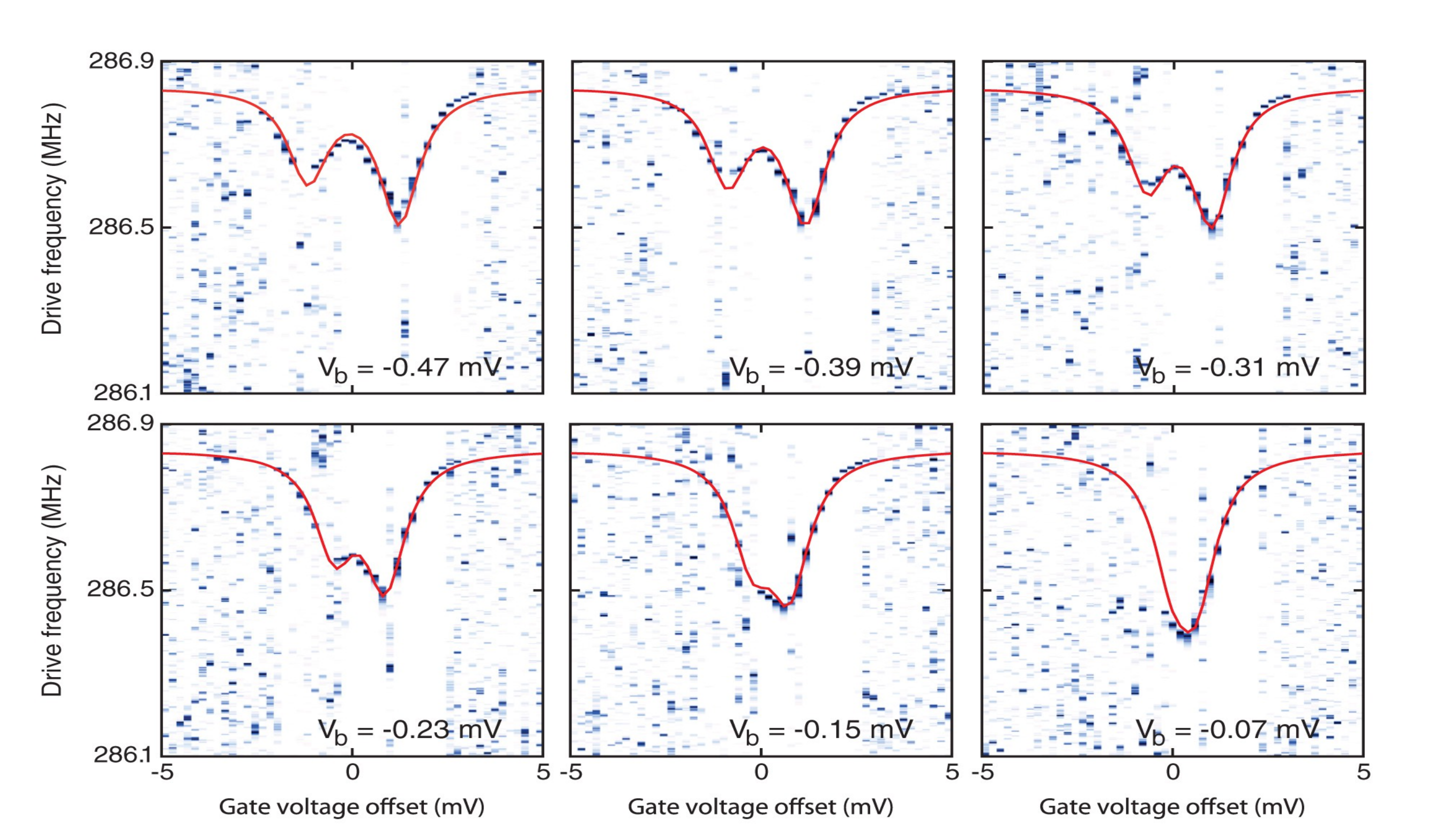

Coulomb-induced nonlinearity

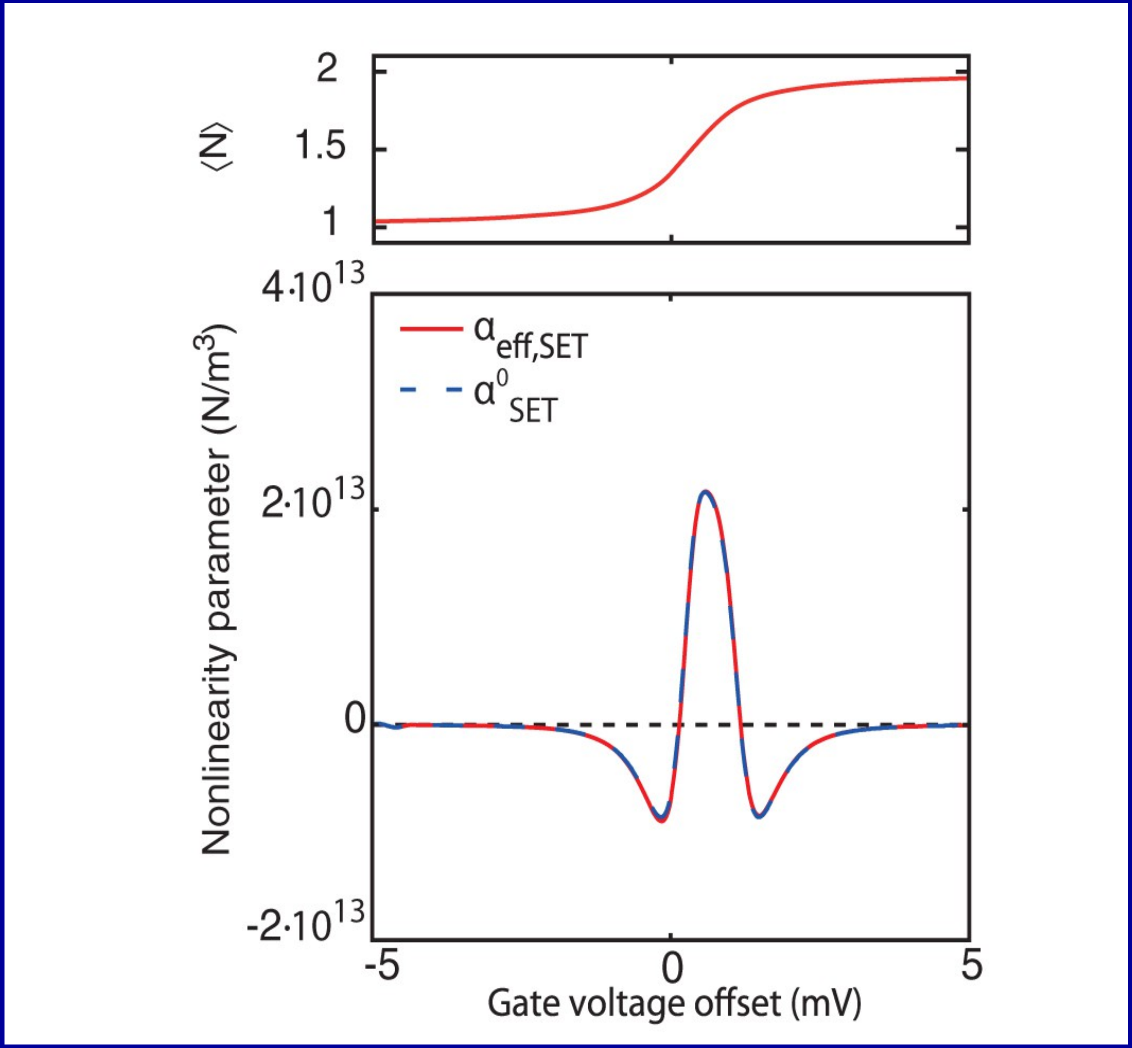

$$F[x] = -\Delta k x - \beta x^2 - \alpha x^3$$

Coulomb-induced damping

$$\frac{\omega_0}{Q} = \frac{\omega_0}{Q_0} + \frac{F_{stoch} V_g}{m C_g} \frac{1}{\Gamma_{tot}} \frac{d C_g}{dx} \frac{\partial \langle N \rangle}{\partial V_g}$$

O. Usmani, YMB, and Yu. V.Nazarov, PRB **75**, 195312 (2007)
F. Pistolesi, YMB, and I. Martin, PRB **78**, 085127 (2008)

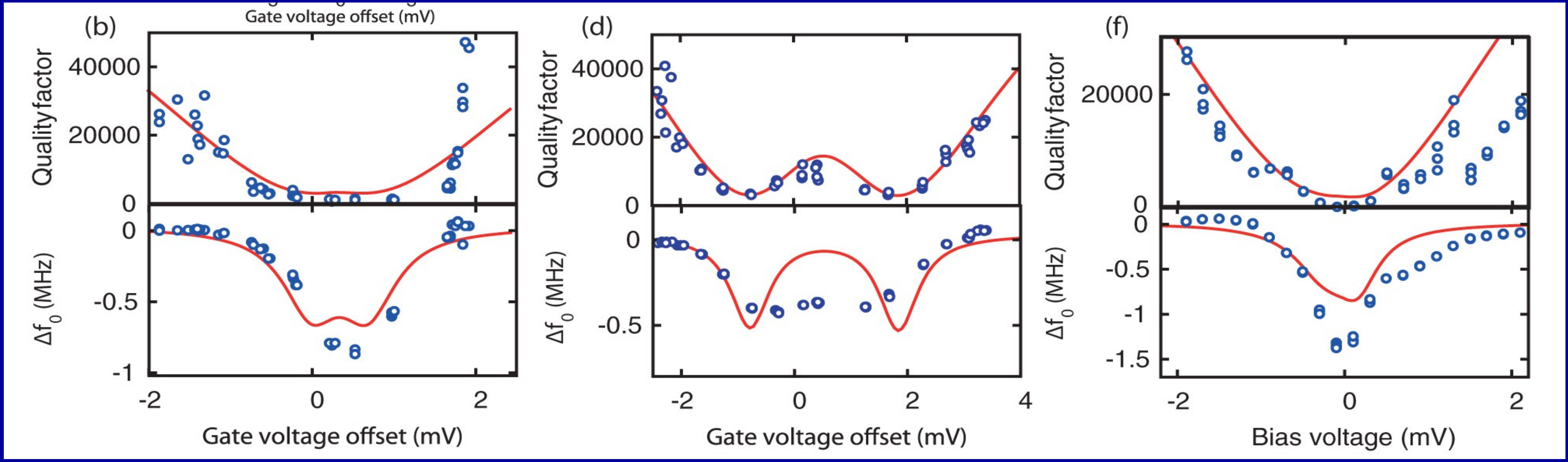

Backaction in SET coupled to a resonator

$P_n(x,v,t)$ - obeys master equation

x – position
v - velocity

O. Usmani, YMB, Yu. V. Nazarov, PRB **75**, 195312 (2007)

$$\frac{\partial P_n}{\partial t} + \left(v\frac{\partial}{\partial x} + \frac{\partial}{\partial v}\frac{F}{M} \right) P_n = St[P]$$

$$F(x,v) = -M\omega^2 x - M\gamma v + Fn$$

Adiabaticity: reduce to Fokker-Planck equation

$$\frac{\partial P}{\partial t} + v\frac{\partial P}{\partial x} - \omega^2 x \frac{\partial P}{\partial v} - \left[\frac{\omega}{Q} + \Psi(x) \right] \frac{\partial}{\partial v}(vP) = D(x)\frac{\partial^2 P}{\partial v^2}$$

Built-in dissipation

Dissipation due to tunneling

Diffusion in velocity space

$$\Psi(x) = \frac{F^2}{M^2}\frac{\Gamma^-(x)\partial_x\Gamma^+(x) - \Gamma^+(x)\partial_x\Gamma^-(x)}{\Gamma_t^3}$$

Strain in graphene

Technische Universiteit Delft

Deformation of a graphene sheet acts at electrons as pseudomagnetic field in the Dirac equation

$$A_x = t\beta(u_{xx} - u_{yy});$$

$$A_y = -2t\beta u_{xy};\ \beta \approx 3$$

H. Suzuura, T. Ando Phys. Rev. B **65**, 235412
F. Guinea, M. I. Katsnelson, M. A. H. Vozmediano Phys. Rev. B **77**, 075422 (2008)

Deformation caused by uniform load:

$$h(r) = \frac{h_0}{R^4}\left(R^2 - r^2\right)^2$$

Deformation caused by local load:

$$h(r) = \frac{h_0}{R^2}\left(\frac{1}{2}\left(R^2 - r^2\right) - r^2 \ln\frac{R}{r}\right)$$

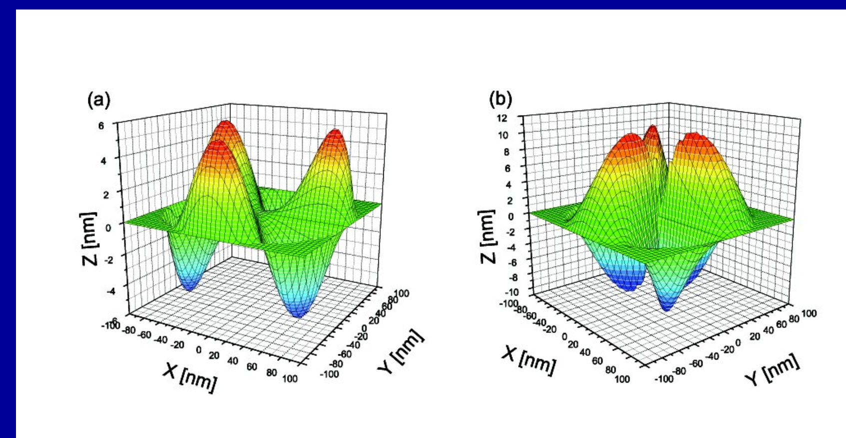

Uniform load   Local load (center)

Dirac equation: with added gauge fields

$$\vec{\sigma}(v_F\vec{p} + \vec{A})\Psi(\vec{r}) = E\Psi(\vec{r})$$

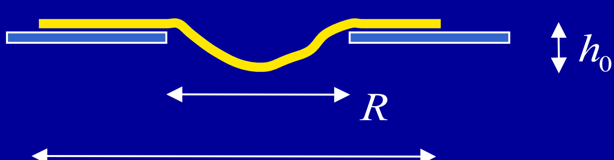

K.-J.Kim, YMB, K.-H.Ahn
Phys. Rev. B **84**, 081401 (2011)

Piezoconductivity in graphene

Deformation:
- Creates strain: pseudomagnetic gauge fields
- Creates density redistribution; the profile needs in principle to be calculated self-consistently

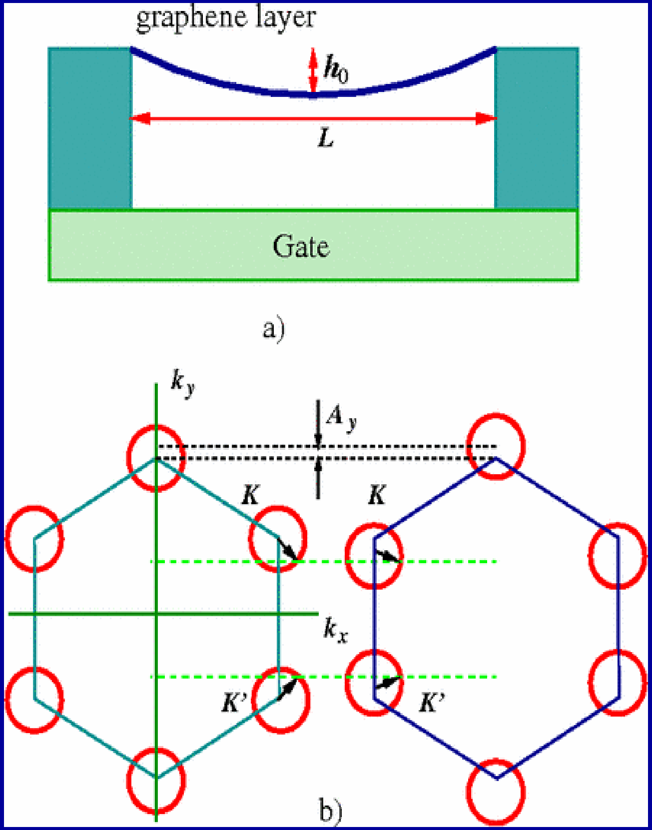

M. Fogler, F. Guinea, M. I. Katsnelson
Phys. Rev. Lett. **101**, 226804 (2008)

Local shift of the Dirac cones:
Predicted metal-insulator transition at certain deformation

Piezoconductivity in graphene

M. V. Medvedyeva and YMB
Phys. Rev. B **83**, 045426 (2011)

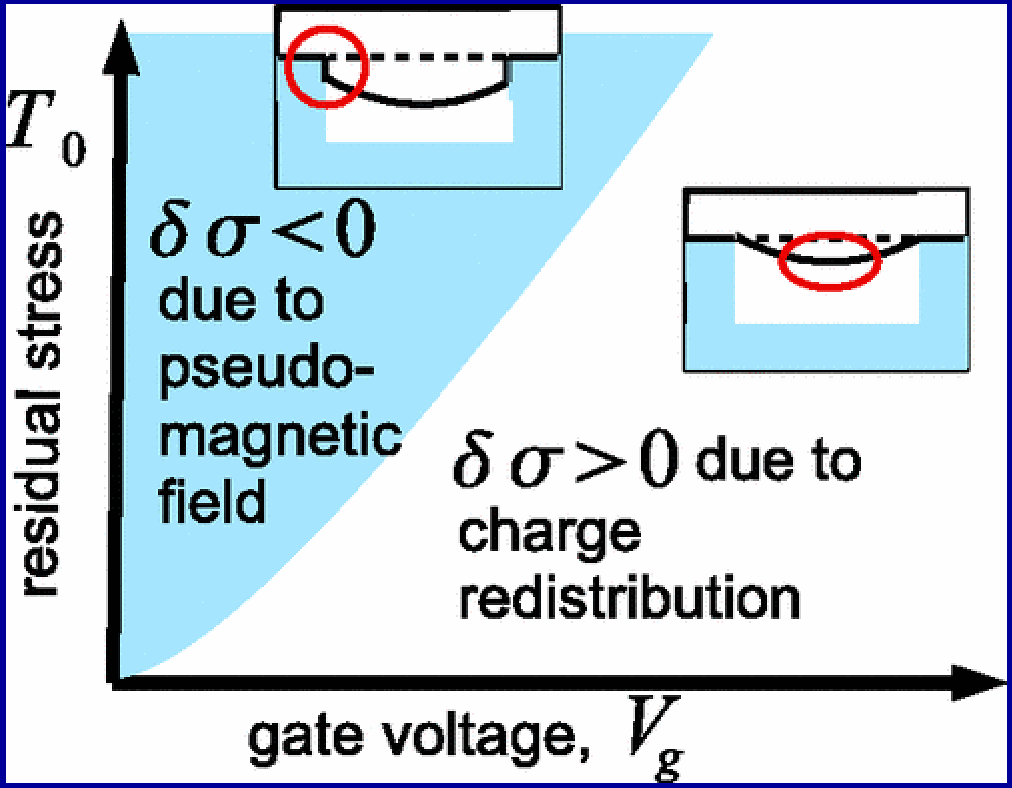

Strain engineering in MoS_2

Wrinkles: large strain difference

A. Castellanos-Gomez, R. Roldán, E. Cappelluti, M. Buschema, F. Guinea, H. S. J. van der Zant, G. A. Steele, Nano Lett. **13**, 5361 (2013)

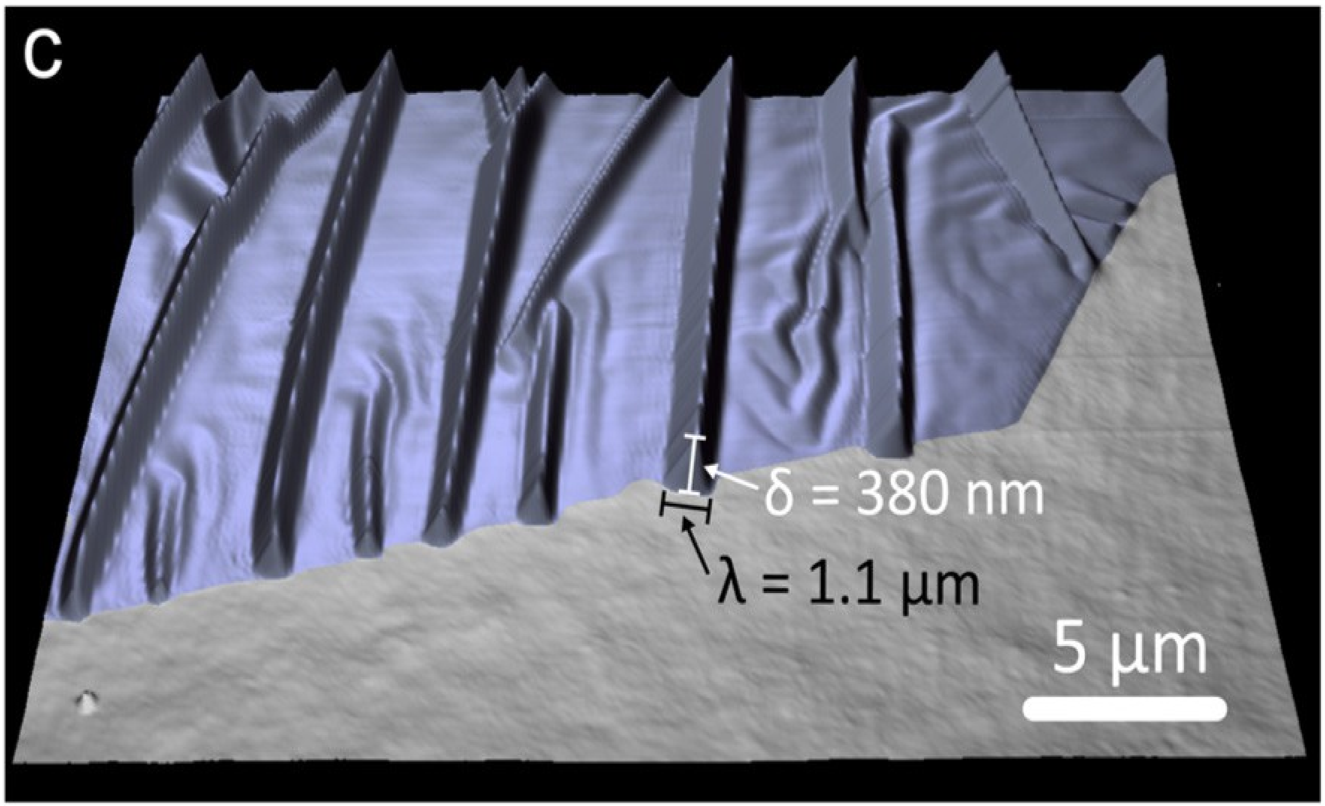

Strain engineering in MoS2

Funneling of excitons

A. Castellanos-Gomez, R. Roldán, E. Cappelluti, M. Buschema, F. Guinea, H. S. J. van der Zant, G. A. Steele, Nano Lett. **13**, 5361 (2013)